

On Flavor Symmetry in Lattice Quantum Chromodynamics

El Hassan Saidi*

1. Lab Of High Energy Physics, Modeling and Simulations, Faculty of Science,
University Mohammed V-Agdal, Av Ibn Battota, Rabat, Morocco
2. Centre Of Physics and Mathematics, CPM- CNESTEN, Morocco

August 21, 2018

Abstract

Using a well established method to engineer non abelian symmetries in superstring compactifications, we study the link between the point splitting method of *Creutz et al* of refs. [1, 2] for implementing flavor symmetry in lattice QCD; and singularity theory in complex algebraic geometry. We show amongst others that *Creutz* flavors for naive fermions are intimately related with toric singularities of a class of complex Kahler manifolds that are explicitly built here. In the case of naive fermions of QCD_{2N} , *Creutz* flavors are shown to live at the poles of real 2-spheres and carry quantum charges of the fundamental of $[SU(2)]^{2N}$. We show moreover that the two *Creutz* flavors in Karsten-Wilczek model, with Dirac operator in reciprocal space of the form $i\gamma_1 F_1 + i\gamma_2 F_2 + i\gamma_3 F_3 + \frac{i}{\sin \alpha} \gamma_4 F_4$, are related with the small resolution of conifold singularity that live at $\sin \alpha = 0$. Other related features are also studied.

Key words: Naive and Karsten-Wilczek fermions, Point splitting method, Toric geometry.

*E-mail: h-saidi@fsr.ac.ma

1 Introduction

Recently M. Creutz and co-workers developed in refs [1, 2] a method to implement flavor symmetry of quarks in lattice QCD by proposing a nice interpretation to the different γ_5 - chiralities of the zeros of the lattice Dirac operator as states of a flavor multiplet. This approach, known as *the point-splitting method*, has been used for various purposes; in particular to identify species in naive and minimally doubled fermions as quark flavors with a non abelian symmetry; and also to define proper flavored-mass terms to extract the index in the spectral flow [3]; see also [4]-[16] for related issues.

On the other hand, one of the lessons learnt from the link between the gauge theory of elementary particles and superstrings is the way to engineer non abelian symmetries for both gauge invariance and flavors [17, 18]. The engineering of these symmetries has been shown to be a smart key to approach the low energy limit of superstrings; especially in dealing with Calabi-Yau compactifications of type II superstrings with branes wrapping cycles [19, 20, 21, 22, 23]. These compactifications involve singular internal manifolds with local singularities leading remarkably to a geometric engineering of the continuous symmetries that we see at low energies [24, 25, 26].

The principal aim of this paper is work out explicitly the link between the point-splitting method of Creutz and collaborators; and the geometric engineering of symmetries by using singularity theory of complex geometry. For concreteness, we will focuss on specific models of lattice QCD namely the Karsten-Wilczek fermions and the naive ones; but our construction is general and applies as well for other fermions. Among our results, we mention too particularly the two following things.

1) the zero modes of the Dirac operator D_{naive} for naive fermions on 2d-dimension lattice \mathcal{L}_{2d} are associated with *toric singularities* [19, 27, 28, 29] of some Kahler manifolds \mathcal{K}_d to be constructed explicitly in section 3. The unit cell \mathcal{C} in the reciprocal lattice $\tilde{\mathcal{L}}_{2d}$ turn out to be exactly the real base Δ_d of the toric graph of the corresponding complex Kahler manifold \mathcal{K}_d . To make an idea on this strange link, recall that the expression of D_{naive} reads in the reciprocal space like

$$D_{naive} = \sum_{l=1}^{2d} i\gamma_l \sin p_l \tag{1.1}$$

with γ_l the hermitian $2^d \times 2^d$ gamma matrices satisfying the Clifford algebra in $2d$ -dimensions. The zeros of this periodic matrix operator, which are located at $\sin p_l = 0$, that is at $p_l = 0$ and $p_l = \pi \bmod{2\pi}$; may be remarkably thought of as the north and south poles of a real 2-sphere \mathbb{S}^2 ; a property that let understand that the Creutz flavors has much to do with the local patches of \mathbb{S}^2 ; see details given in section 3 and eqs(7.6-7.7) of appendix for further explicit relations. We will see throughout this study that D_{naive} can be also viewed as the antihermitian part of the complex matrix operator

$$\mathcal{D} = \sum_{l=1}^{2d} \frac{z_l}{\zeta_l} \gamma_l \quad (1.2)$$

where $(z_l, \zeta_l) \sim (\lambda z_l, \lambda \zeta_l)$, with arbitrary non zero λ , are homogeneous complex coordinates parameterizing the complex projective line $CP^1 \sim \mathbb{S}^2$. This manifold has two toric singularities effectively located at the north and south poles of \mathbb{S}^2 and given, in spherical coordinates $(x, y, z) = (\sin \theta \cos \varphi, \sin \theta \sin \varphi, \cos \varphi)$, by the solutions of $\sin \theta = 0$.

2) The two zero modes of the Dirac for 4-dimensional Karsten-Wilczek fermions have a different geometric interpretation with respect to those of the naive fermions. In the Karsten-Wilczek case as described in [30, 31, 1, 2], we find that the zeros are intimately related with the *small resolution of the conifold singularity* in complex 3-dimension Kahler manifolds [32, 33, 34, 35]. To exhibit rapidly this link, recall that the Dirac of Karsten-Wilczek fermions reads in reciprocal space like

$$D_{KW} = \sum_{l=1}^3 i\gamma_l \sin p_l + \gamma_4 \frac{i}{\sin \alpha} \left((1 - \cos \alpha) + \sum_{l=1}^4 (1 - \cos p_l) \right) \quad (1.3)$$

Notice that the γ_l - coefficients for the first three terms are exactly as for naive fermions in 4d; and so capture the same geometrical property as for (1.1). The γ_4 - coefficient however has a different structure; it depends on two special things: (i) it is given by the sum over the terms $(1 - \cos p_l)$ that have an interpretation in terms of the stereographic projection of the real 2-sphere; and (ii) it has an extra real and free¹ parameter α showing that D_{KW} is in fact an operator flow with spectral parameter α encoding a remarkable singularity for

$$\sin \alpha = 0 \quad (1.4)$$

¹the original Karsten-Wilczek action corresponds to $\alpha = \frac{\pi}{2}$

which, according to the expansions (2.11-2.12), it may be also interpreted as the mass of a non relativistic mode living near the Dirac points. We show in this study that for $\alpha = 0 \bmod \pi$, this singularity is exactly similar to the singularity of the conifold $T^*\mathbb{S}^3$; and the values $\alpha \neq 0$ corresponds precisely to the small resolution of the conic singularity at $\alpha = 0$.

The presentation is as follows: In section 2, we review briefly the main lines of the point-splitting method of *Creutz* for Karsten-Wilczek (KW) fermions of lattice QCD₄; a similar construction is valid for naive fermions (NF). In section 3, we study in details the link between the zero modes of the Dirac operator of naive fermions of lattice QCD₂ and toric singularities; the extension to higher dimensions is straightforward and so omitted. In section 4, we give some useful tools on singularity theory in complex geometry and work out the link with the Creutz point splitting method. In section 5, we study the relation between the zero modes of the Dirac operator of Karsten-Wilczek fermions and the small resolution of conifold. In section 6, we give a conclusion and comments. In the appendix, we recall some useful relations on stereographic projection of real 2-sphere and its Kahler structure.

2 Point-splitting method of Creutz

In this section, we describe the main lines of the point splitting method of *Creutz* [1] for the case of naive fermions and for the Karsten-Wilczek ones on 4-dimensional lattice with typical Dirac operator in reciprocal space as

$$D_{lattice} = \sum_{l=1}^4 i\gamma_l F_l \quad (2.1)$$

For the naive fermions, the coefficients $F_l = \frac{1}{2i} \{D_{lattice}, \gamma_l\}$ of the gamma matrices are all of same nature; and are given by $F_l = \sin p_l$ with

$$p_l = \frac{k_l}{a} \quad (2.2)$$

For Karsten-Wilczek fermions, the F_l 's are as in eq(1.3); so the difference between $D_{lattice}^{(NF)} \equiv D_{NF}$ and $D_{lattice}^{(KW)} \equiv D_{KW}$ concerns the expression of the component

$$F_4 = \frac{1}{2i} \{D_{KW}, \gamma_4\}. \quad (2.3)$$

In eqs(2.1-2.2), the p_l variables are the phases of the wave functions of the particle along the hopping direction; the k_l 's are the components of the wave vector $\mathbf{k} = (k_1, k_2, k_3, k_4)$ and the number a is the spacing parameter of real lattice. In this section, we will mainly focus on KW fermions because of its richer structure; a similar and straightforward analysis is valid for the naive ones.

2.1 specific features of Karsten-Wilczek fermion

The Karsten-Wilczek fermion is a particular 4- dimensional QCD model living on a hypercubic lattice with a Dirac operator D_{KW} having two fermionic zero modes. In the reciprocal space, the lattice Karsten-Wilczek operator D_{KW} reads as follows

$$D_{KW} = \sum_{l=1}^3 i\gamma_l \sin p_l + \gamma_4 \frac{i}{\sin \alpha} \left(\cos \alpha + 3 - \sum_{l=1}^4 \cos p_l \right), \quad (2.4)$$

where, for simplicity, interactions with link fields have been dropped out.

Special properties of D_{KW}

The operator D_{KW} has some remarkable features; in particular the 3 following ones relevant for our study: (i) it depends on an extra real free parameter α whose geometric interpretation will be studied in details later on. (ii) It is an anti-hermitian operator that follows from the Fourier transform of the tight binding hamiltonian of Karsten-Wilczek fermions [2, 36, 37]. This means, on one hand, that D_{KW} can be imagined as

$$D_{KW} = \frac{1}{2} (D - D^+) \quad (2.5)$$

and, on the other hand, it has a hermitian companion $D^{sym} = \frac{1}{2} (D + D^+)$ that is expected to play some role in the geometric interpretation of the zeros. (iii) Because of the gamma matrices, D_{KW} is 4×4 matrix operator that acts on 4- component spinorial wave functions $\psi(\mathbf{k})$ depending on the wave vectors \mathbf{k} of the hopping particles,

$$\psi(\mathbf{k}) = \begin{pmatrix} \phi_i(\mathbf{k}) \\ \bar{\chi}_i(\mathbf{k}) \end{pmatrix} \quad (2.6)$$

with ϕ_i and $\bar{\chi}_i$ standing respectively for the left $\psi_L = \frac{1}{2} (1 + \gamma_5) \psi$ and the right $\psi_R = \frac{1}{2} (1 - \gamma_5) \psi$ handed of ψ . The latters are 2 component Weyl spinors of $SO(4)$,

$$\phi_i = \begin{pmatrix} \phi_1(\mathbf{k}) \\ \phi_2(\mathbf{k}) \end{pmatrix}, \quad \bar{\chi}_i = \begin{pmatrix} \bar{\chi}_1(\mathbf{k}) \\ \bar{\chi}_2(\mathbf{k}) \end{pmatrix} \quad (2.7)$$

having opposite chiralities; $\gamma_5\psi_L = \psi_L$ and $\gamma_5\psi_R = -\psi_R$. The operator D_{KW} has two zero modes which we denote as $\mathbf{P}^\pm = \alpha\mathbf{K}^\pm$; they are located in the reciprocal space at

$$\mathbf{P}^+ = (0, 0, 0, +\alpha) \quad , \quad \mathbf{P}^- = (0, 0, 0, -\alpha) \quad . \quad (2.8)$$

The propagator $\langle \bar{\psi}(p)\psi(p) \rangle = \frac{D_{KW}}{D_{KW}^2}$ has *coupled simple poles*; by setting $p_1 = p_2 = p_3 = 0$ for simplicity and leaving p_4 free, one can show that this propagator reads as

$$\langle \bar{\psi}(p)\psi(p) \rangle |_{p_1=p_2=p_3=0} = \frac{-i\gamma_4 \cot^2 \frac{\alpha}{2}}{\left(1 - \frac{\sin \frac{p}{2}}{\sin \frac{\alpha}{2}}\right) \left(1 + \frac{\sin \frac{p}{2}}{\sin \frac{\alpha}{2}}\right)} \quad (2.9)$$

Observe by the way that in the limit $\alpha = 0$, the two zeros of eq(2.8) collide at the origin $(0, 0, 0, 0)$ of the reciprocal space. This leads to a double pole and so to a symmetry enhancement to be studied in section 5.

Expansions of D_{KW} near the zero modes

To get the expressions of the Dirac operator near its two zero modes P_μ^\pm , we first set $p_\mu = P_\mu^\pm + q_\mu$ with q_μ small fluctuations around the zeros; then expand D_{KW} in series of q_μ to end with two 4×4 matrix operators that we denote like

$$D_+ = D(p_\mu - P_\mu^+) \quad , \quad D_- = D(p_\mu - P_\mu^-) \quad (2.10)$$

The value of these operators at first orders in q_μ gives the usual Dirac operator in continuum; but with two different kinds of gamma matrix representations γ_μ and γ'_μ . For D_+ , we have at the two leading orders in q_μ

$$D_+ = \sum_{\mu=1}^4 i\gamma_\mu q_\mu + i\gamma_4 \left(\sum_{\mu=1}^4 \frac{(q_\mu)^2}{2 \sin \alpha} \right) + O(q^3) \quad (2.11)$$

where the first term is precisely the Dirac operator of a free particle and the second term could be interpreted as a non relativistic massive mode with mass depending on α . Similarly, we find for D_- ,

$$D_- = \sum_{\mu=1}^4 i\gamma'_\mu q_\mu + i\gamma'_4 \left(\sum_{\mu=1}^4 \frac{(q_\mu)^2}{2 \sin \alpha} \right) + O(q^3) \quad (2.12)$$

but now with different matrices γ'_μ that are related to the previous γ_μ 's as

$$\gamma'_1 = \gamma_1 \quad , \quad \gamma'_2 = \gamma_2 \quad , \quad \gamma'_3 = \gamma_3 \quad (2.13)$$

and

$$\gamma'_4 = -\gamma_4 \quad , \quad \gamma'_5 = -\gamma_5 \quad (2.14)$$

showing that the two zeros (2.8) are not equivalent as they have opposite γ_5 -chiralities. Notice that the relations between γ'_μ and γ_μ can be rewritten into a condensed form like

$$\gamma'_\mu = \Gamma^+ \gamma_\mu \Gamma \quad (2.15)$$

where Γ is a similarity transformation given by $\Gamma = i\gamma_4\gamma_5$ and preserve the Clifford algebra $\{\gamma_\mu, \gamma_\nu\} = \{\gamma'_\mu, \gamma'_\nu\} = 2\delta_{\mu\nu}$. The last feature can be explicitly checked by using the following representation of the gamma matrices

$$\gamma^k = \begin{pmatrix} 0 & -i\sigma^k \\ i\sigma^k & 0 \end{pmatrix} \quad , \quad \gamma^4 = \begin{pmatrix} 0 & I \\ I & 0 \end{pmatrix} \quad (2.16)$$

with σ^k standing for the usual 2×2 Pauli matrices and

$$\gamma^5 = \begin{pmatrix} I & 0 \\ 0 & -I \end{pmatrix} \quad , \quad \Gamma = \begin{pmatrix} 0 & -iI \\ iI & 0 \end{pmatrix} \quad (2.17)$$

from which we learn amongst others that $\Gamma^+ = \Gamma$ and $\Gamma^+\Gamma = I_{4 \times 4}$.

2.2 the point splitting method

The point splitting method of Creutz [1, 2] identifies the two *inequivalent* species of the KW fermions that are associated with the operators D_+ and D_- as two independent flavors denoted as u and d . Each flavor field is defined so that the associated fermion propagator, namely $\langle \bar{u}(p) u(p) \rangle$ and $\langle \bar{d}(p) d(p) \rangle$, includes only a single and simple pole. Recall that the propagator of KW fermions has coupled poles (2.9) having the typical form

$$\langle \bar{\psi}(p) \psi(p) \rangle |_{p_1=p_2=p_3=0} = \frac{2C}{(Z-1)(Z+1)} \quad (2.18)$$

with some number C . These coupled simple poles at $Z = \pm 1$ can be split in terms of two isolated simple poles by using the relation

$$\frac{2C}{(Z-1)(Z+1)} = \frac{C}{Z-1} - \frac{C}{Z+1} \quad (2.19)$$

Following [1, 2], the point splitting method to get the flavor $u(\mathbf{p})$ living in the neighborhood of P_μ^+ can be done by multiplying the wave function $\psi(\mathbf{p})$ by a factor that

removes the other pole at P_μ^- . The same procedure can be done for the flavor $d(\mathbf{p})$. This procedure leads to the fields

$$\begin{aligned} u(\mathbf{p} - \alpha \mathbf{e}_4) &= \frac{1}{2} \left(1 + \frac{\sin p_4}{\sin \alpha} \right) \psi(\mathbf{p}) \\ d(\mathbf{p} + \alpha \mathbf{e}_4) &= \frac{1}{2} \left(1 - \frac{\sin p_4}{\sin \alpha} \right) \Gamma \psi(\mathbf{p}) \end{aligned} \quad (2.20)$$

with $\Gamma = i\gamma_4\gamma_5$; and are thought of as the components of an SU(2) flavor doublet,

$$\Psi(\mathbf{p}) = \begin{pmatrix} u(\mathbf{p} - \alpha \mathbf{e}_4) \\ d(\mathbf{p} + \alpha \mathbf{e}_4) \end{pmatrix} \quad (2.21)$$

Here $\mathbf{e}_1, \mathbf{e}_2, \mathbf{e}_3, \mathbf{e}_4$ stand for the basis vectors in the 4-dimensional reciprocal space. In the doubler representation Ψ , the usual chiral matrix γ_5 acting on ψ gets promoted to the tensor product

$$\gamma_5 \otimes \tau^3, \quad \tau^3 = \begin{pmatrix} 1 & 0 \\ 0 & -1 \end{pmatrix} \quad (2.22)$$

together with

$$\gamma_5 \psi \rightarrow \begin{pmatrix} \gamma_5 & 0 \\ 0 & -\gamma_5 \end{pmatrix} \Psi \quad (2.23)$$

where now Ψ is as in (2.21). This point splitting method allows to construct as well mass terms (flavored-mass terms) that assign different masses to the two species. This is done by promoting the 4×4 identity matrix I_4 on ψ as follows

$$I_4 \cdot \psi \rightarrow (I_4 \otimes \tau^3) \Psi = \begin{pmatrix} I_4 & 0 \\ 0 & -I_4 \end{pmatrix} \Psi \quad (2.24)$$

so that

$$\bar{\psi} I_4 \psi \rightarrow \bar{\Psi} (I_4 \otimes \tau^3) \Psi \quad (2.25)$$

which up on substituting (2.21) leads to, on one hand, to

$$\bar{\Psi} (I_4 \otimes \tau^3) \Psi = \bar{u}u - \bar{d}d \quad (2.26)$$

and by help of (2.20) to

$$\bar{u}u - \bar{d}d = \frac{\sin p_4}{\sin \alpha} \bar{\psi} \psi, \quad \bar{u}u + \bar{d}d = \bar{\psi} \psi \quad (2.27)$$

A similar analysis is valid for naive fermions; for more details see below and [2]. In what follows, we study the link between the point splitting method of Creutz and a class of singular complex Kahler manifolds. We first consider the case of naive fermions in 2-dimensional lattice as a matter to illustrate the idea and also to introduce some useful tools; then we turn to the KW model.

3 Naive fermions and toric singularities

In this section we show that the point splitting method for naive fermions (NF) is intimately associated with toric singularities of a particular class of toric manifolds. For the example of 2-dimensional naive fermions on which we focuss below, the corresponding toric manifold is precisely given by the complex projective surface

$$\mathcal{S} = CP^1 \times CP^1 \tag{3.1}$$

made of two CP^1 copies. Recall that the complex projective line CP^1 is isomorphic the usual real 2-sphere S^2 and therefore \mathcal{S} is given by the real 4-dimensional compact manifold $S^2 \times S^2$ [38]. We show also that the first Brillouin zone modded by \mathbb{Z}_2 symmetry of the Dirac operator is nothing but the toric graph of $CP^1 \times CP^1$.

3.1 the naive D_{NF} operator and toric manifolds

To exhibit the link between the zeros of the Dirac operator of naive fermions and toric singularities, let us focus on the simple case of a 2-dimensional lattice with Dirac operator D_{NF} in reciprocal space given by the following field matrix,

$$D_{NF} = i\gamma_1 \sin p_1 + i\gamma_2 \sin p_2 \tag{3.2}$$

with the phases (p_1, p_2) related to the wave vector components (k_1, k_2) as in eq(2.2); that is $p_1 = ak_1, p_2 = ak_2$. The extension to higher dimensions is straightforward.

3.1.1 explicit features of D_{NF} in QCD_2

First notice that to make contact between the zeros of D_{NF} and the usual singularities of complex algebraic geometry, we need to identify a complex operator \mathcal{D} that is associated with D_{NF} and capturing the same physical features as those carried by (3.2). In

particular, it has to be valued in the Clifford algebra in same manner as D_{NF} ;

$$\mathcal{D} = \gamma_1 \mathcal{F}_1(z_1, z_2) + \gamma_2 \mathcal{F}_2(z_1, z_2) \quad (3.3)$$

and has to live on same complex surface parameterized by local coordinates (z_1, z_2) with $\mathcal{F}_1(z_1, z_2)$ and $\mathcal{F}_2(z_1, z_2)$ having the same zeros as D_{NF} .

To build this complex operator, we start by analyzing some useful properties of D_{NF} that are behind the point splitting method. These features are of two kinds: those manifestly exhibited on (3.2); and others ones implicit. Here, we consider the manifest properties of D_{NF} ; the implicit ones will be given in next subsection.

From eq(3.2), we learn that D_{NF} has 3 remarkable and manifest properties:

(1) it is an anti-hermitian operator

$$D_{NF}^+ = -D_{NF} \quad (3.4)$$

and so it can be put into the form

$$D_{NF} = \frac{1}{2} (D - D^+) \quad (3.5)$$

with

$$D = \gamma_1 e^{ip_1} + \gamma_2 e^{ip_2}. \quad (3.6)$$

This feature means also that D_{NF} has a partner given by

$$D^{(sym)} = \frac{1}{2} (D + D^+) \quad (3.7)$$

that turns out to be helpful in looking for a geometric interpretation of the origin of the splitting method of Creutz.

(2) D_{NF} is generally non linear in (p_1, p_2) as it depends on the $\sin p_l$'s; but its expansion near the zeros

$$p_l = 0, \pi$$

has a linear behavior precisely given by the Dirac operator in continuum namely

$$i\gamma_1 p_1 + i\gamma_2 p_2. \quad (3.8)$$

This property is also required by lattice QCD in the continuous limit.

(3) D_{NF} is periodic in both p_1 and p_2 variables; a property that allows to restrict the analysis in the reciprocal space to the fundamental surface of the 2-dimensional momentum

space

$$-\pi \leq p_l \leq \pi \quad , \quad -b\pi \leq k_l \leq b\pi \quad (3.9)$$

with $b = \frac{1}{a}$ the spacing parameter of the reciprocal lattice; see also fig 1.

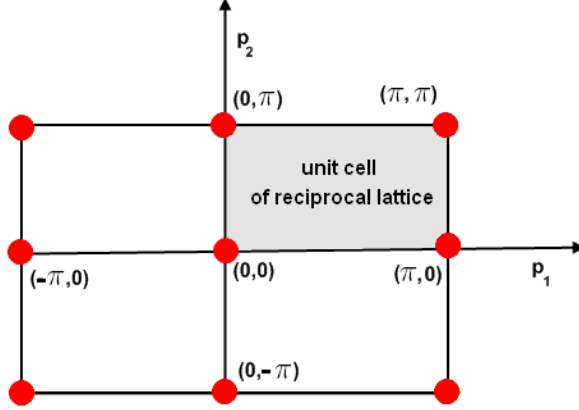


Figure 1: fundamental domain in reciprocal space. \mathbb{Z}_2 symmetry splits this domain into 4 unit cells. The vertices describe the zeros of D_{naive} of QCD_2 fermions; they are also the fix points of \mathbb{Z}_2 .

3.1.2 implicit features of D_{NF}

The D_{NF} given by eq(3.2) has also non manifest features; one of them is that it behaves as an odd operator under the \mathbb{Z}_2 transformation in the momentum space

$$(p_1, p_2) \rightarrow (-p_1, -p_2), \quad (k_1, k_2) \rightarrow (-k_1, -k_2) \quad (3.10)$$

This property allows to restrict the analysis on D_{NF} further to

$$0 \leq p_l \leq \pi \quad , \quad 0 \leq k_l \leq b\pi \quad (3.11)$$

and to which we refer to as unit cell; see fig 1. Later on, we will show that this unit cell is precisely the toric graph of the complex projective surface $CP^1 \times CP^1$ with shrinking 1-cycle on edges and 2-cycle at the vertices. This feature is related to the fact the two zeros of the $\sin p$'s of (3.2) can be interpreted as the north and south poles of a real 2-sphere with coordinates

$$x = \sin p \cos \varphi, \quad y = \sin p \sin \varphi, \quad z = \cos p \quad (3.12)$$

with φ generating the circle \mathbb{S}_φ^1

$$x^2 + y^2 = \rho^2, \quad \rho = \sin p \quad (3.13)$$

For $p = 0$, this circle \mathbb{S}_φ^1 shrinks to the north pole N located at

$$(x, y, z) = (0, 0, 1) \quad (3.14)$$

and for $p = \pi$ it shrinks to the south pole S at

$$(x, y, z) = (0, 0, -1) \quad (3.15)$$

The variation of the radius $\rho = \sin p$ of the circle \mathbb{S}_φ^1 in terms of the phase of the particle is depicted on fig 2. Another implicit feature of D_{NF} concerns the linking of the point

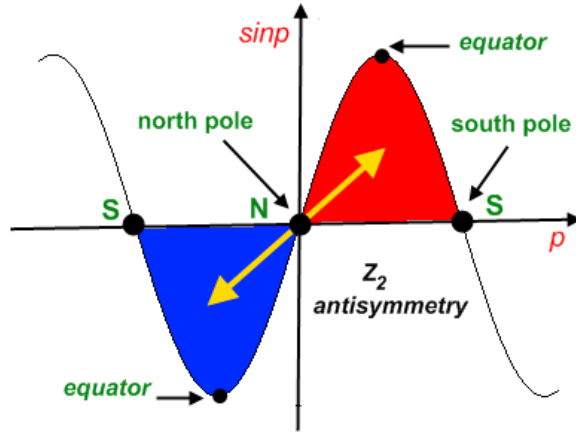


Figure 2: zeros of $\sin p$ as north and south poles of a real 2-sphere; parallel circle at the equatorial plane shrinks at the poles N and S.

splitting method to singularity theory in complex geometry. The complex expression (3.6) leading to D_{NF} looks a very particular quantity since the natural complex extension of D_{NF} would be like

$$\mathbf{D} = z_1\gamma_1 + z_2\gamma_2, \quad (3.16)$$

which, by requiring $|z_1| = |z_2| = 1$, one recovers eq(3.6). However, this complex extension cannot play the role of \mathcal{D} given by eq(3.3). The expression (3.16) destroys a main property of naive fermions since one loses a basic information about the number of zeros of the operator D_{NF} . This means that eq(3.16) is not the exact complex extension

of D_{NF} . Contrary to (3.2) which has 4 zeros, the operator \mathbf{D} has only one zero located at the origin

$$(z_1, z_2) = (0, 0) \tag{3.17}$$

of the complex surface with local coordinates (z_1, z_2) . A careful inspection shows that the exact complex extension of D_{NF} encoding all data on the zeros of D_{NF} should be as follows:

$$\mathcal{D} = \frac{z_1}{\zeta_1} \gamma_1 + \frac{z_2}{\zeta_2} \gamma_2 \tag{3.18}$$

where $(z_i, \zeta_i) \in \mathbb{C} - \{(0, 0)\}$. Notice that this complex operator \mathcal{D} is invariant under the gauge symmetry

$$\begin{aligned} (z_1, \zeta_1) &\rightarrow (\lambda z_1, \lambda \zeta_1) \\ (z_2, \zeta_2) &\rightarrow (\mu z_2, \mu \zeta_2) \end{aligned} \tag{3.19}$$

with λ and μ two non zero complex number generating the $\mathbb{C}^* \times \mathbb{C}^*$ symmetry group. From this view, the operator $\mathbf{D} = z_1 \gamma_1 + z_2 \gamma_2$ appears as a particular case of (3.18) and is recovered by fixing ζ_1 and ζ_2 as follows:

$$\zeta_1 = 1 \quad , \quad \zeta_2 = 1 \tag{3.20}$$

The others zeros of the naive fermions are given by working out the full set of solutions of $\mathcal{D} = 0$; this is done below.

3.2 Zeros of complexified naive \mathcal{D} and point splitting method

We first study the zeros of \mathcal{D} by using the homogeneous complex coordinates $(z_1, \zeta_1, z_2, \zeta_2)$ of the complex surface \mathcal{S} ; then we give the link between the patches of \mathcal{S} and the point splitting method.

3.2.1 the 4 zeros of \mathcal{D}

The conditions (3.20) on the complex variables ζ_1 and ζ_2 are well known relations in complex projective geometry; they correspond precisely to a particular gauge fixing of the $\mathbb{C}^* \times \mathbb{C}^*$ gauge symmetry of \mathcal{D}

$$\begin{aligned} (z_1, \zeta_1) &\rightarrow (z'_1, \zeta'_1) = (\lambda z_1, \lambda \zeta_1) \\ (z_2, \zeta_2) &\rightarrow (z'_2, \zeta'_2) = (\mu z_2, \mu \zeta_2) \end{aligned} \tag{3.21}$$

Being arbitrary non zero complex numbers, one may use this arbitrariness to make diverse particular choices of λ and μ . One of these choices is given by the example

$$\lambda\zeta_1 = 1 \quad , \quad \mu\zeta_2 = 1 \tag{3.22}$$

leading to the following local coordinate patch of the surface \mathcal{S}

$$\begin{aligned} (z'_1, \zeta'_1) &= (z, 1) \quad , \quad z = \frac{z_1}{\zeta_1} \\ (z'_2, \zeta'_2) &= (w, 1) \quad , \quad w = \frac{z_2}{\zeta_2} \end{aligned} \tag{3.23}$$

These relations teach us that the complex variables $(z_1, \zeta_1, z_2, \zeta_2)$ are *homogeneous* coordinates that parameterize the complex projective surface

$$\mathcal{S} = CP^1 \times CP^1, \tag{3.24}$$

embedded in the complex space \mathbb{C}^4 . They tell us moreover that (z_1, ζ_1) and (z_2, ζ_2) are respectively the complex coordinates parameterizing the complex projective curves CP^1 of the complex surface (3.24).

Notice that, along with (3.22), there are also 3 other possible and independent choices of the gauge parameters λ and μ ; they lead to 3 other local patches of the complex surface \mathcal{S} ; they will be given later on. Notice also that in the language of real geometry, the manifold \mathcal{S} can be thought of as given by the 4-real dimensional compact space $\mathcal{S} = \mathbb{S}^2 \times \mathbb{S}^2$ which can be viewed as

$$\mathcal{S} = \mathbb{S}_f^2 \times \mathbb{S}_b^2 \tag{3.25}$$

describing the fibration of a real 2-sphere \mathbb{S}_f^2 fibered on the base 2-sphere \mathbb{S}_b^2 .

The complex operator \mathcal{D} has 4 manifest zeros located at

$$\left(z_1, \frac{1}{\zeta_1}, z_2, \frac{1}{\zeta_2} \right) = \begin{cases} (0, 1, 0, 1) \\ (0, 1, 1, 0) \\ (1, 0, 0, 1) \\ (1, 0, 1, 0) \end{cases} \tag{3.26}$$

in agreement with (3.6). These 4 zeros are precisely located at the north N and south S poles of the spheres $\mathbb{S}_f^2 \times \mathbb{S}_b^2$ namely

$$(N_f, N_b), \quad (N_f, S_b), \quad (S_f, N_b), \quad (S_f, S_b) \tag{3.27}$$

where live as well toric singularities; for technical details see section 4.

3.2.2 point splitting method

Invariance of \mathcal{D} under the gauge symmetry (3.20) allows to make appropriate choices of local coordinate patches \mathcal{U} of the complex surface $\mathcal{S} = CP^1 \times CP^1$ without affecting the physical properties carried by \mathcal{D} . It happens that there are 4 main possible and independent local coordinate patches

$$\mathcal{U}_I, \quad \mathcal{U}_{II}, \quad \mathcal{U}_{III}, \quad \mathcal{U}_{IV} \tag{3.28}$$

with the intersection property

$$\mathcal{U}_I \cap \mathcal{U}_{II} \subseteq \mathbb{C} \quad , \quad \mathcal{U}_{III} \cap \mathcal{U}_{IV} \subseteq \mathbb{C} \tag{3.29}$$

These patches are also in one to one correspondence with the 4 possible gauge fixing conditions of the $\mathbb{C}^* \times \mathbb{C}^*$ symmetry

$$\begin{aligned} \mathcal{U}_I & : \quad \lambda\zeta_1 = 1 \quad , \quad \mu\zeta_2 = 1 \\ \mathcal{U}_{II} & : \quad \lambda\zeta_1 = 1 \quad , \quad \mu z_2 = 1 \\ \mathcal{U}_{III} & : \quad \lambda z_1 = 1 \quad , \quad \mu\zeta_2 = 1 \\ \mathcal{U}_{IV} & : \quad \lambda z_1 = 1 \quad , \quad \mu z_2 = 1 \end{aligned} \tag{3.30}$$

For example, on the coordinate patch \mathcal{U}_I of the complex surface $\mathcal{S} = CP^1 \times CP^1$, which is also equivalent to just setting

$$\mathcal{U}_I : \quad \zeta_1 = 1, \quad \zeta_2 = 1 \tag{3.31}$$

and thinking about z_1 and z_2 as free local complex coordinates, the gauge symmetry $\mathbb{C}^* \times \mathbb{C}^*$ is completely fixed; and the complexified Dirac operator \mathcal{D} reduces to eq(3.16) with a zero at $(0, 1, 0, 1)$. This property shows that the splitting method of the four zeros of (3.2) is intimately related with the gauge fixing choices (3.30). In other words, there is a one to one correspondence between the 4 Creutz flavors and the Dirac operator $\mathcal{D}(\mathcal{U})$ on the 4 local patches of $\mathcal{S} = \mathbb{S}^2 \times \mathbb{S}^2$ as given in the following table,

patch of \mathcal{S}	$(z_1, \zeta_1) \in CP^1_{(1)}$	$(z_2, \zeta_2) \in CP^1_{(2)}$	\mathcal{D}
\mathcal{U}_I	$(z_1, 1)$	$(z_2, 1)$	$\mathcal{D}_I = z_1\gamma_1 + z_2\gamma_2$
\mathcal{U}_{II}	$(z_1, 1)$	$(1, \zeta_2)$	$\mathcal{D}_{II} = z_1\gamma_1 + \frac{1}{\zeta_2}\gamma_2$
\mathcal{U}_{III}	$(1, \zeta_1)$	$(z_2, 1)$	$\mathcal{D}_{III} = \frac{1}{\zeta_1}\gamma_1 + z_2\gamma_2$
\mathcal{U}_{IV}	$(1, \zeta_1)$	$(1, \zeta_2)$	$\mathcal{D}_{IV} = \frac{1}{\zeta_1}\gamma_1 + \frac{1}{\zeta_2}\gamma_2$

On each local patch \mathcal{U} of the complex surface \mathcal{S} , the complex operator $\mathcal{D}(\mathcal{U})$ has a simple zero where live a degenerate *toric symmetry*.

Below, we give details on this kind of singularities whose typical graphic representation is depicted in figures 3 and 4.

4 Toric singularities and Creutz Flavors

Here we show, by using explicit tools, that Creutz flavors in naive fermions live exactly at the toric singularities of the complex surface $CP^1 \times CP^1$; the extension to higher dimensions follows the same rule. To that purpose, we start by recalling some useful tools on toric symmetry and toric singularities; then we make the link with Creutz flavors.

4.1 two examples of toric singularities

Here, we give two examples of toric manifolds and toric singularities as a way to illustrate the general idea. We first consider the simple case of \mathbb{C} , the set of complex numbers; then we describe the case of the complex projective line CP^1 . The latter is one of the basic objects in dealing with toric geometry; in particular in building toric graphs and studying toric singularities.

1) *the complex line* $\mathbb{C} \sim \mathbb{R}^2$

The complex line \mathbb{C} is the simplest example of toric manifolds. To exhibit the toric

structure of \mathbb{C} and build the corresponding toric graph [19, 29, 27, 28], it is convenient to think about the complex coordinate $z = x + iy$ as

$$z = |z| e^{i\varphi} \tag{4.1}$$

with $|z| = \sqrt{x^2 + y^2} \in \mathbb{R}^+$ and $\tan \varphi = \frac{y}{x}$. By using this representation, the complex line \mathbb{C} may be viewed as the fibration of a circle \mathbb{S}^1 over the real half line \mathbb{R}^+ ; i.e:

$$\mathbb{C} \sim \mathbb{R}^+ \times \mathbb{S}^1 \tag{4.2}$$

This non compact complex line admits a natural $U(1)$ action operating as

$$z \rightarrow z' = ze^{i\theta} \quad \Leftrightarrow \quad \varphi \rightarrow \varphi + \theta \tag{4.3}$$

with a fixed point at $z = 0$. In toric geometry, the complex line \mathbb{C} is represented by a toric graph given by the half-line $\mathbb{R}^+ = [0, \infty[$, corresponding to $|z|$, above which there is a circle of radius $r = r(|z|)$. The toric graph of \mathbb{C} is depicted in fig 3; the circle of the

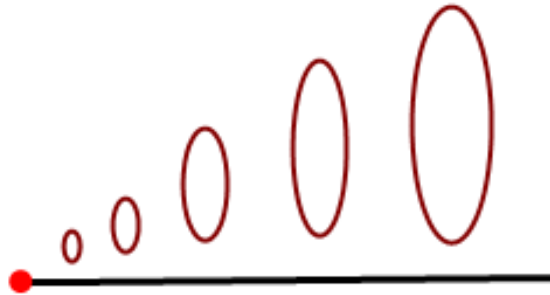


Figure 3: toric graph of \mathbb{C} viewed as a half-line $\mathbb{R}^+ = [0, \infty[$ with a circle on top which shrinks at the origin.

fibration shrinks to zero at the end of the half-line where live the fix point of the toric action;

$$z = z' = 0. \tag{4.4}$$

2) the projective line $CP^1 \sim \mathbb{S}^2$

The projective line CP^1 is one of the basic objects in drawing toric graphs of toric manifolds; it is then useful to have some extensive details on this compact complex curve, which in the real geometry language, describes precisely the real 2-sphere \mathbb{S}^2 considered

in section 3.1.2. First notice that \mathbb{S}^2 may be realized in various, but equivalent, manners depending on the targeted features. We have the three following realizations of \mathbb{S}^2 :

(i) by embedding it in the real 3-euclidian space as usual like $(x_1)^2 + (x_2)^2 + (x_3)^2 = \varrho^2$ with x_i standing for the coordinates of \mathbb{R}^3 .

(ii) by thinking about it as the coset group manifold

$$\mathbb{S}^2 \sim SU(2)/U(1) \quad (4.5)$$

which is realized by using two complex variables w_+, w_- constrained as [39, 40]

$$|w_+|^2 + |w_-|^2 = \xi, \quad \xi \geq 0, \quad (4.6)$$

together with the gauge identification

$$w_+ \equiv e^{i\varphi} w_+, \quad w_- \equiv e^{-i\varphi} w_- \quad (4.7)$$

Equation (4.6) fixes one degree of the real 4 degrees of freedom leaving three free ones; the second relation reduces this number down to 2. The real parameter ξ in (4.6) is the Kahler parameter of the real 2-sphere; it controls its volume. Notice also that the variables (w_+, w_-) form two states of an $SU(2)$ doublet with opposite $U(1)$ charges as shown on the following relation

$$\begin{pmatrix} w_+ \\ w_- \end{pmatrix} \rightarrow e^{i\varphi\tau^3} \begin{pmatrix} w_+ \\ w_- \end{pmatrix}, \quad \tau^3 = \begin{pmatrix} 1 & 0 \\ 0 & -1 \end{pmatrix} \quad (4.8)$$

This feature can be seen by setting

$$\begin{aligned} w^\alpha &= \begin{pmatrix} w_+ \\ w_- \end{pmatrix}, & w_\alpha &= \begin{pmatrix} w_- \\ -w_+ \end{pmatrix} \\ \bar{w}_\alpha &= \begin{pmatrix} \bar{w}_+ \\ \bar{w}_- \end{pmatrix}, & \bar{w}^\alpha &= \begin{pmatrix} -\bar{w}_- \\ \bar{w}_+ \end{pmatrix} \end{aligned} \quad (4.9)$$

with $\bar{w}_\alpha = \overline{(w^\alpha)}$ where the index α is raised and lowered by help of the antisymmetric 2×2 metric tensor $\varepsilon_{\alpha\beta}$ of spinors. As such, we have

$$w^\alpha \bar{w}_\alpha = \varepsilon_{\alpha\beta} w^\alpha \bar{w}^\beta \quad (4.10)$$

which upon using the above relations leads to precisely $|w_+|^2 + |w_-|^2$ showing that it is invariant under $SU(2)$ transformations. We also have $w^\alpha w_\alpha = \varepsilon_{\alpha\beta} w^\alpha w^\beta = 0$ and similarly for the complex conjugates.

(iii) the 2-sphere \mathbb{S}^2 may be as well realized in terms of the projective line CP^1 which is given by the compactification of the complex line. We have [40]

$$CP^1 = \mathbb{C}^2 / \mathbb{C}^* \tag{4.11}$$

with \mathbb{C}^* standing for the symmetry action $(z, \zeta) \rightarrow (\lambda z, \lambda \zeta)$. The toric graph of the projective line is given by fig 4. The projective line has also a $U(1)$ toric action in terms

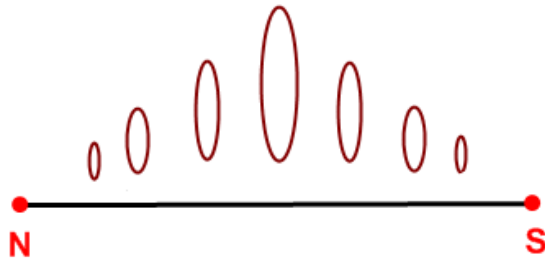


Figure 4: toric graph of $CP^1 \sim \mathbb{S}^2$ which can be viewed as an interval $[N, S]$ with a circle on top. The circle fiber shrinks to zero size at the ends N and S.

of which the 2-sphere can be represented as an interval $[N, S]$ times a circle \mathbb{S}^1 that shrinks at the two ends N and S, corresponding to north and south poles of the sphere. The coordinate ς on the interval is a function of $|z|$, which upon using the Fubini-Study metric, reads as [29],

$$\varsigma = \frac{\eta |z|^2}{1 + |z|^2} \tag{4.12}$$

and runs from 0 to η defining the length of the interval $[N, S]$ and so the size of the 2-sphere. Notice that in dealing with CP^1 ; one has to distinguish between the homogeneous coordinates² (Z_1, Z_0) and the affine ones that corresponds to working in a local patch.

4.2 the complex surface $CP^1 \times CP^1$

This is a complex 2- (real 4-) dimensional compact manifold that can be described by 4 complex homogeneous variables

$$(z_1, \zeta_1, z_2, \zeta_2) \in \frac{\mathbb{C}^2 \times \mathbb{C}^2}{\mathbb{C}^* \times \mathbb{C}^*} \tag{4.13}$$

²In eq(3.21) the homogenous (Z_1, Z_0) are denoted as (z_1, ζ_1)

obeying the identifications

$$\begin{aligned} (z_1, \zeta_1) &\rightarrow (\lambda z_1, \lambda \zeta_1) \\ (z_2, \zeta_2) &\rightarrow (\mu z_2, \mu \zeta_2) \end{aligned} \quad (4.14)$$

where λ and μ are two non zero complex numbers. This complex surface has a $U^2(1)$ toric action, consisting of the $U^4(1)$ action on the phases of (z_i, ζ_i) modulo the action of the diagonal $U(1) \times U(1)$ which act trivially on $CP^1 \times CP^1$. Being a toric manifold, $CP^1 \times CP^1$ may be viewed as the fibration

$$CP^1 \times CP^1 \sim \Delta_2 \times T^2 \quad (4.15)$$

with real 2-dimensional base Δ_2 and a fiber T^2 . The toric diagram of this manifold is given by the tensor product of the toric graphs of the two CP^1 's; the resulting polytope is as in fig 5; the base Δ_2 is a parallelogram $[ABCD]$ with vertices

$$\begin{aligned} A = (0, 1, 0, 1) \quad , \quad C = (1, 0, 0, 0) \\ B = (1, 0, 0, 1) \quad , \quad D = (1, 0, 1, 0) \end{aligned} \quad (4.16)$$

and should be associated with the unit cell in the reciprocal space given by fig 1. Let us describe rapidly the construction of this toric graph. In the coordinate patch where $\zeta_1 = \zeta_2 = 1$, we can consider a basis of the $U^2(1)$ action to consist of

$$(z_1, 1, z_2, 1) \rightarrow (z'_1, 1, z'_2, 1) = (z_1 e^{i\theta_1}, 1, z_2 e^{i\theta_2}, 1) \quad (4.17)$$

The fixed point of the θ_1 action consists of the complex line $(0, 1, z_2, 1)$ describing a local coordinate patch of a projective line CP^1 to which we refer as the copy $CP^1_{(2)}$ parameterized by $\frac{z_2}{\zeta_2} = z_2$. Similarly the fixed point of the θ_2 action is given by $(z_1, 1, 0, 1)$; it is a local patch of a $CP^1_{(1)}$ parameterized by $\frac{z_1}{\zeta_1} = z_1$. The intersection of the two lines is given by the point

$$(0, 1, 0, 1) \quad (4.18)$$

which is a fix point of both θ_1 and θ_2 actions. The same situation takes place for the other patches; for instance if we work in the coordinate patch where $z_1 = \zeta_2 = 1$, we can consider a basis of the $U^2(1)$ action to consist of

$$(1, \zeta_1, z_2, 1) \rightarrow (1, \zeta'_1, z'_2, 1) = (1, \zeta_1 e^{i\phi_1}, z_2 e^{i\theta_2}, 1) \quad (4.19)$$

The fix point of the ϕ_1 action consists of $(1, 0, z_2, 1)$ and describes the projective line $CP^1_{(2)}$ parameterized by $\frac{z_2}{\zeta_2} = z_2$. While the fixed point of the θ_2 action is a CP^1 parameterized by $\frac{z_1}{\zeta_1} = \frac{1}{\zeta_1}$; it is precisely the $CP^1_{(1)}$; but taken in the local coordinate patch $(1, \zeta_1)$.

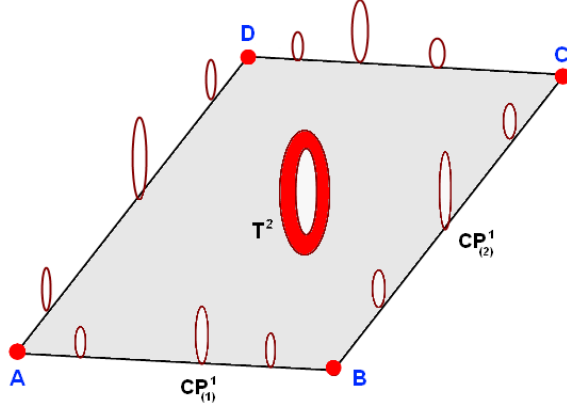


Figure 5: toric graph of the complex surface $CP^1 \times CP^1 \sim \mathbb{S}^2 \times \mathbb{S}^2$. On the edges a 1-cycle of the 2-torus shrinks leaving \mathbb{S}^1 . At the 4 vertices both the 1-cycles of T^2 shrink to zero; these points correspond to fix points of the $U^2(1)$ toric action.

4.3 Creutz Flavors

First recall that for QCD₂ naive fermions, the Dirac operator $D_{NF} = i\gamma_1 \sin p_1 + i\gamma_2 \sin p_2$ has four zeros in reciprocal space located at $\mathbf{P}_{m_1, m_2} = (P_1^{(m_1)}, P_2^{(m_2)})$ with:

$$P_1^{(m_1)} = m_1\pi, \quad P_2^{(m_2)} = m_2\pi, \quad m_l = 0, 1 \quad (4.20)$$

These 4 zeros are also the fix points of the \mathbb{Z}_2 anti-symmetry of D_{NF}

$$(p_1, p_2) \rightarrow (-p_1, -p_2) \quad (4.21)$$

they form the vertices of a unit cell in the reciprocal space as depicted in fig 1. At these 4 vertices of the unit cell which we denote as

$$\begin{aligned} A &= (P_1^{(0)}, P_2^{(0)}) & , & & B &= (P_1^{(1)}, P_2^{(0)}) \\ C &= (P_1^{(0)}, P_2^{(1)}) & , & & D &= (P_1^{(1)}, P_2^{(1)}) \end{aligned} \quad (4.22)$$

both the Dirac operator coefficients $\sin p_1$ and $\sin p_2$ vanish; while on the 4 edges

$$[AB], \quad [BC], \quad [CD], \quad [DA] \quad (4.23)$$

only one of the two $\sin p_l$'s of D_{naive} that vanishes. Moreover, inside the surface of the cell, $\sin p_1$ and $\sin p_2$ are both of them non zero exactly as in for the toric graph of

$$CP^1 \times CP^1.$$

Now, expanding D_{naive} near each one of the 4 zeros (4.22) by setting $p_l = P_l^{(m_l)} + q_l$ and using the identity

$$\sin\left(q_l + P_l^{(m_l)}\right) = \sin q_l \cos P_l^{(m_l)} + \cos q_l \sin P_l^{(m_l)} \quad (4.24)$$

we get 4 kinds of Dirac operators $D_{(m_1, m_2)}$ in the continuum. These expansions read collectively as

$$D_{(m_1, m_2)} \simeq \gamma_{(m_1)}^1 q_1 + \gamma_{(m_2)}^2 q_2 + O(q^2) \quad (4.25)$$

with $\gamma_{(m_1)}^1$ and $\gamma_{(m_2)}^2$ related to the standard ones γ^l like,

$$\gamma_{(m_1)}^1 = (-)^{m_1} \gamma^1, \quad \gamma_{(m_2)}^2 = (-)^{m_2} \gamma^2 \quad (4.26)$$

and obeying as well the same Clifford algebra. The above relations can be also written in terms of the following similarity transformations

$$\gamma_{(m_1)}^1 = \Gamma_{(m_1, 0)}^+ \gamma^1 \Gamma_{(m_1, 0)}, \quad \gamma_{(m_2)}^2 = \Gamma_{(0, m_2)}^+ \gamma^2 \Gamma_{(0, m_2)} \quad (4.27)$$

with

$$\Gamma_{(m_1, m_2)} = (\gamma^1)^{m_2} (\gamma^2)^{m_1} \quad (4.28)$$

Applying the point splitting method to this model by identifying the 4 *inequivalent* species associated with the operators $D_{(m_1, m_2)}$ as 4 independent flavors, we end with the 4 Creutz flavors

$$\psi_{(m_1 m_2)} = \begin{pmatrix} \psi_{(00)} & \psi_{(01)} \\ \psi_{(10)} & \psi_{(11)} \end{pmatrix} \quad (4.29)$$

with

$$\psi_{(m_1 m_2)} \sim \Gamma_{(m_1 m_2)} \psi \left(p_1 - P_1^{(m_1)}, p_2 - P_2^{(m_2)} \right) \quad (4.30)$$

Moreover, thinking about $\sin p_1$ and $\sin p_2$ as the radii of two circles as in eq(3.13); it follows that the unit cell of fig 1 is precisely the real base of the toric graph of $CP^1 \times CP^1$ given by fig 5.

Furthermore, rewriting the 4 zeros (4.20)

$$(P_1, P_2) = (0, 0), (\pi, 0), (\pi, 0), (\pi, \pi) \quad (4.31)$$

in terms of the wave vectors $(K_1, K_2) = (bP_1, bP_2)$, with b given by the inverse of the real lattice spacing parameter ($b = \frac{1}{a}$), we obtain the following parallelogram

$$(K_1, K_2) = (0, 0), (b\pi, 0), (b\pi, 0), (b\pi, b\pi) \quad (4.32)$$

with area

$$\mathcal{A} = \pi^2 b^2 \quad (4.33)$$

Notice that in the infrared limit $b \rightarrow 0$, the area of the unit cell in reciprocal lattice shrinks and the 4 zeros collide leading to an $SU(2) \times SU'(2)$ singularity. This means that the Creutz multiplet $\psi_{(m_1 m_2)}$ transforms in the $(\frac{1}{2}, \frac{1}{2})$ representation of $SU(2) \times SU'(2)$.

5 KW fermions and Conifold

We begin by recalling the Dirac operator D_{KW} of the KW fermions on 4-dimensional lattice. This is anti-hermitian 4×4 matrix operator given by (2.4) which, for convenience, we rewrite it as

$$D_{KW} = \sum_{l=1}^4 i\gamma_l F_l \quad (5.1)$$

with $F_l = \sin p_l$ for $l = 1, 2, 3$ as for naive fermions; and the fourth component F_4 given by

$$F_4 = \frac{1}{\sin \alpha} \left(\cos \alpha + 3 - \sum_{l=1}^4 \cos p_l \right) \quad (5.2)$$

Generally, this operator depends on three basic objects namely: (1) the 4 gamma matrices $\gamma_1, \gamma_2, \gamma_3, \gamma_4$ satisfying the euclidian Clifford algebra $\gamma_\mu \gamma_\nu + \gamma_\nu \gamma_\mu = 2\delta_{\mu\nu}$ leading to the remarkable property

$$(D_{KW})^2 = -I_4 \left(\sum_{l=1}^4 F_l^2 \right), \quad D_{KW} D_{KW}^+ = -(D_{KW})^2 \quad (5.3)$$

where I_4 is the 4×4 identity matrix. (2) the real 4 phases $e^{ip_1}, e^{ip_2}, e^{ip_3}, e^{ip_4}$ of the wave functions of the particle propagating along the directions towards the first nearest neighbors in the real 4d-hypercubic lattice; and (3) the free real parameter α showing that the KW operator (2.4) is in fact a one- parameter flow operator

$$D_{KW} = D(\alpha). \quad (5.4)$$

with spectral parameter α .

5.1 zeros of D_{KW} as fix points of \mathbb{Z}_2 symmetry

The operator D_{KW} has some remarkable features that allows to interpret the point splitting method of Creutz in terms of a blown up singularity in complex geometry. Four useful features for this study are collected below:

i) D_{KW} is a periodic operator in the reciprocal space variables p_1, p_2, p_3, p_4 and also in the spectral parameter α . So the variation of the p_l 's and α can be restricted to a particular period which can be taken as

$$p_l, \alpha \in]-\pi, \pi] \quad , \quad \text{mod } 2\pi \quad (5.5)$$

ii) D_{KW} is moreover odd under the \mathbb{Z}_2 parity transformation reversing simultaneously the sign of the phase variables p_l and the spectral parameter α as follows

$$(p_1, p_2, p_3, p_4; \alpha) \rightarrow (-p_1, -p_2, -p_3, -p_4; -\alpha) \quad (5.6)$$

This \mathbb{Z}_2 anti-symmetry allows to restrict further the domain (5.5) down to

$$p_l, \alpha \in [0, \pi] \quad (5.7)$$

We will refer to this fundamental domain in the reciprocal space as the unit cell; this is a 4-dimensional hypercube with volume, in terms of the spacing parameter a of the real lattice, given by $\frac{\pi^4}{a^4}$.

iii) the operator D_{KW} admits also another property that has no analogue in the case of naive fermions; it is singular for $\alpha = \alpha_{sg}$ with

$$\alpha_{sg} = 0, \pi, \quad \text{mod } 2\pi \quad (5.8)$$

as explicitly shown on the expression of F_4 (5.2). This feature can be also exhibited by computing the leading terms of the expansion of F_4 for α close to α_{sg} . In the case $\alpha \sim 0$, we have

$$F_4 \simeq \frac{1}{\alpha} \left(4 - \sum_{l=1}^4 \cos p_l \right) + \frac{\alpha}{6} \left(1 - \sum_{l=1}^4 \cos p_l \right) + O(\alpha^3) \quad (5.9)$$

whose leading term has a pole at $\alpha = 0$. Notice that at this pole, the function F_4 diverges as far as $\sum_{l=1}^4 (1 - \cos p_l) \neq 0$.

iv) In the case where $\alpha \neq \alpha_{sg}$, the operator D_{KW} has two simple zero modes located at

$$\mathbf{P}_{\pm} = (0, 0, 0, \pm\alpha) = \pm\alpha\mathbf{e}_4 \quad (5.10)$$

with $\mathbf{e}_4 = (0, 0, 0, 1)$ standing for the fourth direction of the reciprocal space. These zeros, which are related by the \mathbb{Z}_2 anti-symmetry (5.6), show that:

- Karsten-Wilczek fermions have non trivial wave phases only along the \mathbf{e}_4 - direction,
- the two zeros collide in the limit $\alpha \rightarrow 0$ giving a rank two degenerate zero:

$$\lim_{\alpha \rightarrow 0} \mathbf{P}_+ = \lim_{\alpha \rightarrow 0} \mathbf{P}_- = (0, 0, 0, 0) \quad (5.11)$$

Observe also that for those p_l phases that are in the nearby of the zeros \mathbf{P}_\pm , say for instance $p_l = \mathbf{P}_+ + q_l$ with small q_l , the coefficient F_4 reads as

$$F_4 = \frac{1}{\sin \alpha} \left(3 - \sum_{l=1}^3 \cos q_l + \cos \alpha (1 - \cos q_4) + \sin \alpha \sin q_4 \right) \quad (5.12)$$

and expands, at first order in q , like $F_4 \simeq q_4 + O(q_l^2, \alpha)$.

5.2 F_4 as a resolved conifold singularity

By writing the Dirac operator as

$$D_{KW} = +i\gamma_1 \sin p_1 + i\gamma_2 \sin p_2 + i\gamma_3 \sin p_3 + \frac{i}{\sin \alpha} \mathcal{F}_4 \quad (5.13)$$

with \mathcal{F}_4 given by the α -dependent function

$$\mathcal{F}_4(\alpha) = \left(4 - \sum_{l=1}^4 \cos p_l \right) - (1 - \cos \alpha) \quad (5.14)$$

we learn that the zeros of the $\sin p_l$ coefficients along the $\gamma_1, \gamma_2, \gamma_3$ directions are as in the case of naive fermions and so are interpreted in terms of toric singularities as in fig 5. However the two simple zeros of the term \mathcal{F}_4 have a different geometric interpretation; they are associated with the small resolution of the conifold singularity which we prove hereafter.

5.2.1 useful tools on singularities

To get the link between the two zeros of the KW fermions and the small resolution of conifold singularity, it is helpful to start by giving some useful tools on $SU(2)$ and conifold singularities; then turn back to derive the relation with zeros of KW fermions. To this end we will proceed as follows:

- first, we describe briefly the $SU(2)$ singularity and its resolution in terms of a blown up real 2-sphere where the order 2 degenerate zero gets replaced by two simple zeros [17, 18].
- second, we study the conifold singularity together with its complex and Kahler deformations. The latter, known also as the small resolution, uses a blown up 2-sphere to lift the conifold singularity [32, 33, 34, 35]; it is the one related to the zeros of KW fermions.

A) $SU(2)$ singularity

There are various ways to introduce this singularity; the most natural one is given by considering those singular complex surfaces

$$\mathcal{G}(z_1, z_2, z_3) = 0 \tag{5.15}$$

embedded in \mathbb{C}^3 and known as the Asymptotic Locally Euclidian (ALE) space. In this case, the shape of the complex surface \mathcal{G} near the singularity is described by the following complex algebraic relation

$$\mathcal{G}(z_1, z_2, z_3) = (z_1)^2 + (z_2)^2 + (z_3)^2 \tag{5.16}$$

which is invariant under the \mathbb{Z}_2 symmetry $z_l \rightarrow z'_l = -z_l$. This discrete symmetry has a fix point $z'_l = z_l$ at the origin $(z_1, z_2, z_3) = (0, 0, 0)$ where live indeed an $SU(2)$ singularity. Up on performing the variable change

$$u = z_1 + iz_2, \quad v = z_1 - iz_2, \quad z = z_3 \tag{5.17}$$

we can bring the above relation to the familiar form,

$$uv = z^2 \tag{5.18}$$

with fix point of the \mathbb{Z}_2 symmetry at $(u, v, z) = (0, 0, 0)$. Recall that by $SU(2)$ singularity, we mean that the equation $\mathcal{G} = 0$ and its differential $d\mathcal{G} = 0$ have the same zeros which in this example is precisely the fix point of the \mathbb{Z}_2 symmetry namely $(z_1, z_2, z_3) = (0, 0, 0)$. Notice also that the complex surface (5.16) is a manifold belonging to an interesting class of Kahler manifolds known as *toric manifolds*. These manifolds, introduced in section 4, admit toric actions and are nicely represented by toric diagrams. In the case of the ALE

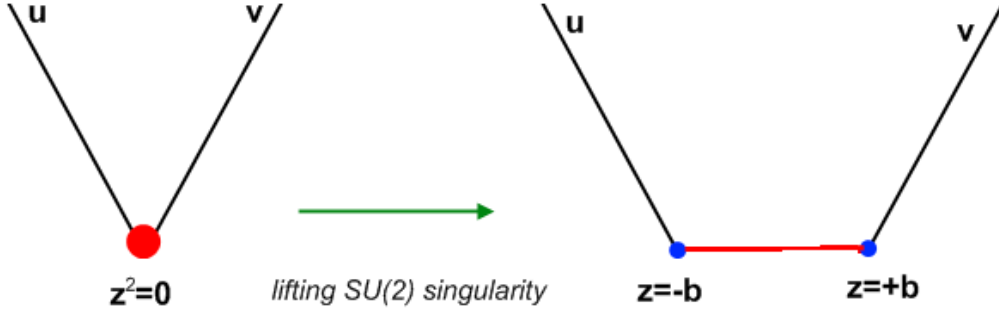


Figure 6: on left the $SU(2)$ singularity at the origin. On right its resolution; the singular point $z = 0$ has been replaced by a complex projective line.

space with $SU(2)$ singularity, the corresponding toric graph and its deformation are as in fig 6.

From the structure of eq(5.16), the complex 2- dimension surface $\mathcal{G}(z_1, z_2, z_3) = 0$ is nothing but the tangent bundle of the 2-sphere $T^*\mathbb{S}^2$ which may be thought of as given by the fibration $\mathbb{S}^2 \times \mathbb{R}^2$. This feature can be viewed by working with the real coordinates; by using $z_l = x_l + iy_l$ and putting back into (5.16), we obtain the two real equations

$$\sum_{l=1}^3 (x_l^2 - y_l^2) = 0 \quad , \quad \sum_{l=1}^3 x_l y_l = 0 \quad (5.19)$$

describing the fibration $T^*\mathbb{S}^2 \simeq \mathbb{S}^2 \times \mathbb{R}^2$. The compact part of this manifold obtained by setting $y_l = 0$; the reduced relation describes a real 2-sphere \mathbb{S}^2 ; but with vanishing volume; that is a singular 2-sphere:

$$\sum_{l=1}^3 x_l^2 = 0 \quad (5.20)$$

The singular surface (5.16) may be smoothed by giving a non zero volume to the above singular \mathbb{S}^2 ; this is achieved by replacing (5.16) by the deformed relation

$$z_1^2 + z_2^2 + z_3^2 = \beta^2 \quad (5.21)$$

where β is an arbitrary non zero number. Rewriting this deformed relation as

$$z_1^2 + z_2^2 + (z_3 - \beta)(z_3 + \beta) = 0 \quad (5.22)$$

one sees that the double zero at $z_3^2 = 0$ is now splitted into two simple zeros located at

$$z_3 = +\beta, \quad z_3 = -\beta \quad (5.23)$$

This is almost what happens with the zeros of the KW fermions which are located in the real 4-dimensional reciprocal space at

$$p_4 = +\alpha, \quad p_4 = -\alpha \quad (5.24)$$

the role of the parameter β is played by the free parameter α . We will turn to this relation in next subsection; in due time notice that in toric geometry language, the $SU(2)$ singularity of the ALE space corresponds to the shrinking of 2-torus at the origin; the deformation corresponds to blowing up a 2-sphere at the singularity. So the two degenerate zeros living at the fix point get splitted and pushed towards the north and south poles of the blown up sphere as in fig 4. The blown up breaks the $SU(2)$ living at the singularity down to its $U(1)$ subgroup

$$SU(2) \rightarrow U(1) \quad (5.25)$$

B) 3d- conifold singularity

The complex 3d-conifold we are interested in here is given by the complex 3-dimensional affine variety generally defined by the complex algebraic equation

$$G(u, v, z, w) = uv - zw = 0 \quad (5.26)$$

describing a singular complex 3-dimensional hypersurface embedded in \mathbb{C}^4 . By using the following change of variables

$$\begin{aligned} u &= z_1 + iz_2, & v &= z_1 - iz_2, & w &= -z_4 + iz_3 \\ z &= z_1 + iz_2, & z &= z_4 + iz_3 \end{aligned} \quad (5.27)$$

this complex relation can be brought to the diagonal form

$$(z_1)^2 + (z_2)^2 + (z_3)^2 + (z_4)^2 = 0. \quad (5.28)$$

Viewed as a real 6-dimensional affine variety embedded into the euclidian space \mathbb{R}^8 , the real relations that define the conifold are obtained by substituting $z_l = x_l + iy_l$ back into (5.28); this gives

$$\sum_{l=1}^4 (x_l^2 - y_l^2) = 0, \quad \sum_{l=1}^4 x_l y_l = 0 \quad (5.29)$$

with compact part given by the singular real 3-sphere \mathbb{S}^3

$$\sum_{l=1}^4 x_l^2 = 0 \quad (5.30)$$

The non compact part, parameterized by the y_l variables, is given by the real 3-dimensional space \mathbb{R}^3 which, in spherical coordinates, can be also viewed as given by the fibration of a real 2-sphere on the half line like $\mathbb{R}^+ \times \mathbb{S}^2$. So the conifold may be thought of as

$$\mathbb{R}^+ \times \mathbb{S}^2 \times \mathbb{S}^3 \quad (5.31)$$

The geometry of this real 6-dimensional conifold can be therefore imagined as a cone in \mathbb{R}^8 with base $\mathbb{S}^2 \times \mathbb{S}^3$ and top at the origin as heuristically depicted by in fig 7-a.

On the other hand, by using the Hopf fibration $\mathbb{S}^3 \sim \mathbb{S}^1 \times \mathbb{S}^2$, which in Lie groups language corresponds to

$$SU(2) = U(1) \times \frac{SU(2)}{U(1)} \quad (5.32)$$

and using as well the toric fibration of the complex line $\mathbb{C} = \mathbb{R}^+ \times \mathbb{S}^1$, one may also think about the conifold as a complex 3d- toric manifold with the fibration

$$\mathbb{C} \times \mathbb{S}^2 \times \mathbb{S}^2 \sim \mathbb{C} \times CP^1 \times CP^1 \quad (5.33)$$

The defining equations of this complex threefold, whose toric graph is given by fig 7-b, can be obtained from (5.29) by using the variable change

$$\begin{aligned} U_1 &= x_1 + ix_2 \quad , \quad U_2 = x_3 + ix_4 \\ V_1 &= y_1 + iy_2 \quad , \quad V_2 = y_3 + iy_4 \end{aligned} \quad (5.34)$$

to put it into the form

$$\begin{aligned} |U_1|^2 + |U_2|^2 - |V_1|^2 - |V_2|^2 &= 0 \\ U_1 \bar{V}_1 + U_2 \bar{V}_2 + \bar{U}_1 V_1 + \bar{U}_2 V_2 &= 0 \end{aligned} \quad (5.35)$$

These relations may be also obtained from eq(5.26) by setting

$$\begin{aligned} u &= U_1 + iV_1 \quad , \quad z = U_2 - iV_2 \\ v &= \bar{U}_1 + i\bar{V}_1 \quad , \quad w = \bar{U}_2 - i\bar{V}_2 \end{aligned} \quad (5.36)$$

Notice that eqs(5.35) are invariant under the $U(1)$ gauge symmetry

$$\begin{aligned} U'_1 &= e^{i\varphi} U_1 \quad , \quad V'_1 = e^{i\varphi} V_1 \\ U'_2 &= e^{-i\varphi} U_2 \quad , \quad V'_2 = e^{-i\varphi} V_2 \end{aligned} \quad (5.37)$$

which is associated with the \mathbb{S}^1 fiber in the the Hopf fibration of \mathbb{S}^3 . Notice also that the compact part is given by the relation $|U_1|^2 + |U_2|^2 = 0$; and the small resolution of the conifold singularity amounts to substitute it by

$$|U_1|^2 + |U_2|^2 = \xi, \quad U'_1 \equiv e^{i\varphi}U_1, \quad U'_2 \equiv e^{-i\varphi}U_2 \quad (5.38)$$

where the positive number ξ stands for the Kahler parameter of the 2-sphere $\mathbb{S}^2 \sim \mathbb{S}^3/\mathbb{S}^1$. Under this resolution, eqs(5.35) get promoted to

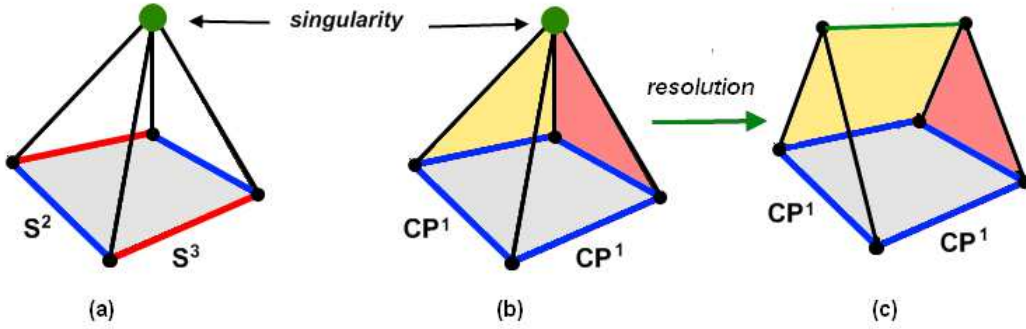


Figure 7: (a) the conifold viewed as $\mathbb{S}^2 \times \mathbb{S}^3 \times \mathbb{R}^+$; the resolution of the singularity can be achieved in 2 ways, either by blowing a 3-sphere or a 2-sphere. (b) the conifold viewed as the toric diagram of $CP^1 \times CP^1 \times \mathbb{C}$. (c) Small resolution of conifold by blowing up the singularity by a CP^1 curve.

$$\begin{aligned} |U_1|^2 + |U_2|^2 - |V_1|^2 - |V_2|^2 &= \xi \\ U_1 \bar{V}_1 + U_2 \bar{V}_2 + \bar{U}_1 V_1 + \bar{U}_2 V_2 &= 0 \end{aligned} \quad (5.39)$$

With these tools at hand we turn to study the zeros of the KW fermions.

5.2.2 the \mathcal{F}_4 term (5.2)

Here, we give the explicit relation between the zeros of the \mathcal{F}_4 term (5.2) and the small resolution of the conifold singularity. To that purpose, notice first that for $\alpha = 0$, we have

$$\mathcal{F}_4(\alpha) |_{\alpha=0} = \sum_{l=1}^4 (1 - \cos p_l) \quad (5.40)$$

The typical terms $(1 - \cos p_l)$ can be seen as $(1 - z_l)$ with $z_l = \cos p_l$ giving the altitude of the shrinking circle $x_l^2 + y_l^2 = \sin^2 p_l$ of the real 2-sphere parameterized by the spherical

coordinates,

$$x_l = \rho_l \cos \varphi_l, \quad y_l = \rho_l \sin \varphi_l, \quad z_l = \cos p_l, \quad (5.41)$$

with $\rho_l = \sin p_l$ and

$$x_l^2 + y_l^2 + z_l^2 = 1. \quad (5.42)$$

Using the standard identities

$$\sin p = 2 \cos \frac{p}{2} \sin \frac{p}{2}, \quad 1 - \cos p = 2 \sin^2 \frac{p}{2} \quad (5.43)$$

we can rewrite the Dirac operator for the KW fermions like

$$D_{KW} = 2i \sum_{l=1}^3 \gamma_l \cos \frac{p_l}{2} \sin \frac{p_l}{2} + \frac{2i}{\sin \alpha} \gamma_4 \mathcal{F}_4 \quad (5.44)$$

with

$$\mathcal{F}_4(p) = \sum_{l=1}^4 \left(\sin \frac{p_l}{2} \right)^2 - \left(\sin \frac{\alpha}{2} \right)^2 \quad (5.45)$$

Setting

$$\begin{aligned} X_l &= \cos \frac{p_l}{2}, & Y_l &= \sin \frac{p_l}{2} \\ A &= \cos \frac{\alpha}{2}, & B &= \sin \frac{\alpha}{2} \end{aligned} \quad (5.46)$$

satisfying the constraint relation

$$X_l^2 + Y_l^2 = 1, \quad A^2 + B^2 = 1 \quad (5.47)$$

we can rewrite the D_{KW} operator like

$$D_{KW} = 2i \sum_{l=1}^3 \gamma_l X_l Y_l + \frac{2i}{\sin \alpha} \gamma_4 \mathcal{F}_4 \quad (5.48)$$

with the \mathcal{F}_4 term along the γ_4 direction as follows

$$\mathcal{F}_4(Y, B) = (Y_1)^2 + (Y_2)^2 + (Y_3)^2 + (Y_4)^2 - B^2 \quad (5.49)$$

Clearly, in the real coordinate frame (Y_1, Y_2, Y_3, Y_4) , the zeros of the \mathcal{F}_4 term describe a real 3-sphere \mathbb{S}^3 of radius $|B|$. So the the limit $B \rightarrow 0$, which by using (5.46) corresponds to the limit $\alpha \rightarrow 0$, describes precisely the vanishing of the volume of a 3-sphere;

$$\mathcal{F}_4(Y, B)|_{B=0} = 0 \quad \Leftrightarrow \quad (Y_1)^2 + (Y_2)^2 + (Y_3)^2 + (Y_4)^2 = 0 \quad (5.50)$$

This shows that the of $\mathcal{F}_4(Y, B)|_{B \neq 0}$ is related to the resolution of a 3-dimensional conifold singularity of fig 7-b.

5.3 \mathcal{F}_4 - term and the complexified D_{KW} operator

Following the same reasoning we have done for naive fermions, one may think about the the antihermitian operator D_{KW} as given by

$$D_{KW} = \frac{D - D^+}{2} \quad (5.51)$$

with

$$D = \sum_{l=1}^3 \gamma_l z_l^2 + \frac{1}{c^2} \gamma_4 (z_1^2 + z_2^2 + z_3^2 + z_4^2 - c^2) \quad (5.52)$$

where the z_l 's are complex variables and c is a priori a complex modulus. Clearly D contains (5.48) and is singular for $c = 0$ as in the case of D_{KW} . Writing this complex operator D like,

$$D = \sum_{l=1}^3 \gamma_l \mathcal{L}_l + \frac{1}{c^2} \gamma_4 \mathcal{L}_4 \quad (5.53)$$

with

$$\begin{aligned} \mathcal{L}_l &= \frac{1}{2} \{\gamma_l, D\} = z_l^2 \\ \mathcal{L}_4 &= \frac{c^2}{2} \{\gamma_4, D\} = (z_1^2 + z_2^2 + z_3^2 + z_4^2 - c^2) \end{aligned} \quad (5.54)$$

Then substituting

$$z_l = x_l + iy_l, \quad c = \xi + i\zeta \quad (5.55)$$

back into (5.52), we get for the first 3 terms $\mathcal{L}_1, \mathcal{L}_2, \mathcal{L}_3$ the generic expression

$$\mathcal{L}_l = (x_l^2 - y_l^2) + 2ix_ly_l \quad (5.56)$$

and for the 4-th the following

$$\mathcal{L}_4 = \frac{\xi - i\zeta}{\xi^2 + \zeta^2} \left(\sum_{l=1}^4 (x_l^2 - y_l^2) - (\xi^2 - \zeta^2) \right) + 2i \frac{\xi - i\zeta}{\xi^2 + \zeta^2} \left(\sum_{l=1}^4 x_ly_l - \xi\zeta \right) \quad (5.57)$$

In the particular case $\xi = 0$, the term \mathcal{L}_4 reduces to

$$\mathcal{L}_4 = \frac{i}{\zeta} \left(\sum_{l=1}^4 (x_l^2 - y_l^2) + \zeta^2 \right) + \frac{2}{\zeta} \sum_{l=1}^4 x_ly_l \quad (5.58)$$

By setting

$$\begin{aligned} u_1 &= x_1 + ix_3, & u_2 &= x_2 + ix_4 \\ v_1 &= y_1 + iy_3, & v_2 &= y_2 + iy_4 \end{aligned} \quad (5.59)$$

we also have

$$\begin{aligned} \mathcal{L}_4 &= \frac{-i}{\zeta} (|v_1|^2 + |v_1|^2 - |u_1|^2 - |u_1|^2 - \zeta^2) \\ &\quad - \frac{2}{\zeta} (u_1 \bar{v}_1 + u_2 \bar{v}_2 + \bar{u}_1 v_1 + \bar{u}_2 v_2) \end{aligned} \quad (5.60)$$

The zeros of \mathcal{L}_4 are obtained by solving the two following relations given by the real and imaginary parts

$$\begin{aligned} |v_1|^2 + |v_1|^2 - |u_1|^2 - |u_1|^2 &= \zeta^2 \\ u_1 \bar{v}_1 + u_2 \bar{v}_2 + \bar{u}_1 v_1 + \bar{u}_2 v_2 &= 0 \end{aligned} \quad (5.61)$$

But these relations are nothing but those describing the resolved conifold (5.39). The compact part of this manifold is given by $|v_1|^2 + |v_1|^2 = \zeta^2$ as given by 7-(c); the non compact part is parameterized by the u_l 's.

6 Conclusion and comment

Motivated by Creutz point splitting method of refs [1, 2], we have learnt in this study two basic things regarding naive and Karsten-Wilczek fermions of lattice QCD. Concerning naive fermions, we have shown that the zeros of the Dirac operator D_{naive} have a geometric interpretation in terms of *toric singularities* of some complex Kahler manifolds that have been explicitly constructed here. The Brillouin zone moded by the \mathbb{Z}_2 antisymmetry (3.10) of the Dirac operator D_{naive} turns out to be exactly the base of the toric fibration of a toric Kahler manifold \mathcal{K} . For instance, in the case of naive fermions of QCD₂, the corresponding toric manifold is precisely the complex surface

$$CP^1 \times CP^1 \sim \mathbb{S}^2 \times \mathbb{S}^2 \quad (6.1)$$

with toric graph given by the fig 5. Moreover seen that the homogeneous coordinates (z, ζ) of each CP^1 form an $SU(2)$ doublet, it follows that the 4 zeros of naive fermions of QCD₂ live at the poles of $\mathbb{S}^2 \times \mathbb{S}^2$ and carry quantum charges of the bi-spinor representation

$$\left(\frac{1}{2}, \frac{1}{2}\right) \quad \text{of} \quad SU(2) \times SU(2) \sim SO(4) \quad (6.2)$$

This result extends straightforwardly to higher dimensions. In QCD₄, the Dirac operator of the naive fermions in the reciprocal space

$$D_{naive} = i\gamma_1 \sin p_1 + i\gamma_2 \sin p_2 + i\gamma_3 \sin p_3 + i\gamma_4 \sin p_4 \quad (6.3)$$

has $2^4 = 16$ zeros located at $\mathbf{P}_{(m_1, m_2, m_3, m_4)} = (P_1^{(m_1)}, \dots, P_4^{(m_1)})$ with

$$\begin{aligned} P_1^{(m_1)} &= m_1\pi, & P_2^{(m_2)} &= m_2\pi, \\ P_3^{(m_3)} &= m_3\pi, & P_4^{(m_4)} &= m_4\pi, \end{aligned} \quad , \quad m_l = 0, 1 \quad (6.4)$$

Because of periodicity of D_{naive} in the wave phases p_l and because of the \mathbb{Z}_2 anti-symmetry changing the signs of these phases, the zeros of the 4 $\sin p_l$'s, which are also fix points of \mathbb{Z}_2 , should be viewed as the vertices of 4d- unit cell in the reciprocal space. This unit cell has 3-dimensional divisors (cubes), 2-dimensional faces (squares), 1-dimensional edges (segments) and vertices (points). On the 3d-divisors one of the 4 $\sin p_l$ vanish while on the 2d- faces two of them vanish. On the edges of the unit cell, 3 of the 4 $\sin p_l$ vanish and at the vertices the 4 $\sin p_l$'s vanish in complete agreement with toric singularities of the toric four-fold

$$CP^1 \times CP^1 \times CP^1 \times CP^1 \quad (6.5)$$

Moreover, the expansions of the Dirac operator near the 16 zeros read in a condensed manner like

$$D_{\mathbf{m}} \simeq \gamma_{(m_1)}^1 q_1 + \gamma_{(m_2)}^2 q_2 + \gamma_{(m_3)}^3 q_3 + \gamma_{(m_4)}^4 q_4 + O(q^2) \quad (6.6)$$

where \mathbf{m} stand for the 4-dimensional integral vector (m_1, m_2, m_3, m_4) with $m_l = 0, 1$; and where the gamma matrices $\gamma_{(m_i)}^i$ are related to the standard ones γ^l as follows

$$\gamma_{(m_i)}^i = (-)^{m_i} \gamma^i \quad (6.7)$$

The wave functions $\Psi_{\mathbf{m}} = \psi(q_{\mathbf{m}})$ near the 2^4 zero modes (6.4) with

$$q_{\mathbf{m}} = (p_1 - P_1^{(m_1)}, p_2 - P_2^{(m_2)}, p_3 - P_3^{(m_3)}, p_4 - P_4^{(m_4)}) \quad (6.8)$$

depend on the values of the integral vector \mathbf{m} capturing the $[SU(2)]^4$ symmetry of the four-fold (6.5). So the waves $\Psi_{\mathbf{m}}$ carry quantum charges of the fundamental representation

$$\left(\frac{1}{2}, \frac{1}{2}, \frac{1}{2}, \frac{1}{2}\right) \quad (6.9)$$

of the group $[SU(2)]^4$.

Concerning the Karsten-Wilcek fermions of lattice QCD₄, we have learnt that the two zero modes of the Dirac operator D_{KW} (1.3) are fix points of the \mathbb{Z}_2 symmetry (5.6). Like for naive fermions, these zeros form an $SU(2)$ doublet and have as well a geometric interpretation in terms of the small resolution of the conifold.

7 Appendix: Features of $\mathbb{S}^2 \sim CP^1$

In this appendix, we collect some useful relations on the real 2-sphere \mathbb{S}^2 . Because of special features, this compact 2-dimensional surface can be approached in various ways; three of them were briefly described in subsection 4.1, eqs(4.4) to (4.12); they are:

$$\begin{aligned}
 (i) & : \mathbb{S}^2 \subset \mathbb{R}^3 \\
 (ii) & : \mathbb{S}^2 \simeq SU(2)/U(1) \\
 (iii) & : \mathbb{S}^2 \simeq CP^1
 \end{aligned}
 \tag{7.1}$$

Our interest into the real 2-sphere; in particular into its Kahler structure and toric representation, is because the north and south poles of \mathbb{S}^2 host the Creutz flavors of naive fermions considered in this paper.

First, notice that the power of the properties of \mathbb{S}^2 comes essentially from its link with the complex projective line and the $SU(2)$ Lie group. To any complex number $z = x+iy \in \mathbb{C}$, represented as (x, y) in the plane \mathbb{R}^2 , one can associate a point (u, v, w) on the unit 2-sphere

$$\mathbb{S}^2 = \{(u, v, w) \in \mathbb{R}^3 \mid u^2 + v^2 + w^2 = 1\}
 \tag{7.2}$$

This mapping is known as the stereographic projection from the unit sphere \mathbb{S}^2 minus the point $N = (0, 0, 1)$ (north³ pole) onto the plane $w = 0$, which we identify with the complex plane with coordinate $z = x + iy$.

To get the explicit relations between the (u, v, w) variables and the planar (x, y) , one projects the point $P = (u, v, w) \in \mathbb{S}^2 - \{N\}$ on to the plane $w = 0$. Straightforward calculations lead to

$$u = \frac{2x}{1+|z|^2} \quad , \quad v = \frac{2y}{1+|z|^2} \quad , \quad w = \frac{|z|^2-1}{1+|z|^2}
 \tag{7.3}$$

with inverse relations as

$$x = \frac{u}{1-w} \quad , \quad y = \frac{v}{1-w}
 \tag{7.4}$$

In the spherical coordinates (θ, φ) with zenith θ and azimuth ϕ variables as $0 \leq \theta \leq \pi$, $0 \leq \varphi \leq 2\pi$; we can combine the u and v coordinates into a complex one like

$$u + iv = \sin \theta e^{i\varphi}, \quad w = \cos \theta
 \tag{7.5}$$

³one may also consider the stereographic projection using the south pole $(0, 0, -1)$.

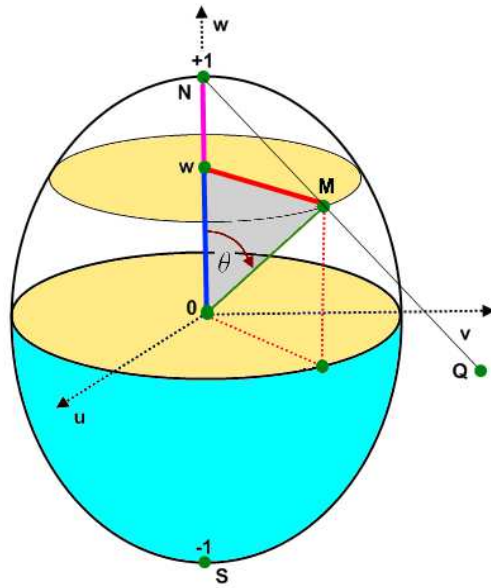


Figure 8: stereographic projection of real 2-sphere using north pole. Recall that the poles of the sphere host Creutz fermions; the coefficient $\sin p_l$ of the Dirac operator of naive fermions are interpreted in terms of the radius $\sin \theta$ of the parallel circle which shrinks at the poles.

This leads to $|u + iv| = \sin \theta$ and shows that the radius $\rho = \sin \theta$ of the parallel circle in \mathbb{S}^2 vanishes at north $\theta = 0$ and south $\theta = \pi$ poles. By setting

$$r = \frac{\sin \theta}{1 - \cos \theta} = \frac{\cos \frac{\theta}{2}}{\sin \frac{\theta}{2}} \quad (7.6)$$

we also have

$$x + iy = r e^{i\varphi}, \quad r = \cot \frac{\theta}{2} \quad (7.7)$$

showing that the singularity at the south pole $\theta = \pi$ is stereographically mapped to the origin of the complex plane; and the singularity at north $\theta = 0$ is mapped to infinity. This property should be compared with the two zeros of the complex ratio $\frac{\xi}{\zeta}$ describing the complex projective line parameterized by the homogeneous coordinates (z, ζ) ; see also eqs(3.18) and 3.26) to make contact with zero modes of the Dirac operator of naive fermions and *Creutz* flavors.

Seen as a Kähler manifold, the metric of the complex projective line follows as a particular case of the Fubini-Study metric of complex n-dimensional projective spaces CP^n ; it reads in the local coordinate patch (chart) $\zeta = 1$ as follow

$$ds^2 = \frac{4}{(1 + |z|^2)^2} dz d\bar{z} \quad (7.8)$$

Automorphisms of the 2-sphere using the (non homogenous) affine coordinate z is given by the mobius transformations

$$z' = \frac{az + b}{cz + d} \quad (7.9)$$

with a, b, c, d four complex numbers constrained as $ad - bc \neq 0$. By using the homogeneous complex coordinates (z, ζ) , this transformation reads also like

$$\begin{pmatrix} z' \\ \zeta' \end{pmatrix} = \begin{pmatrix} a & b \\ c & d \end{pmatrix} \begin{pmatrix} z \\ \zeta \end{pmatrix} \quad (7.10)$$

and shows that (z, ζ) transform indeed as an $SU(2)$ doublet.

Acknowledgement 1 *This work is supported by CNRST under contract URAC09.*

References

- [1] M. Creutz, Minimal doubling and point splitting, PoS: Lattice 2010, 078 (2010) [arXiv:1009.3154],

- [2] Michael Creutz, Taro Kimura, Tatsuhiro Misumi, *Index Theorem and Overlap Formalism with Naive and Minimally Doubled Fermions*, JHEP 1012:041,2010, arXiv:1011.0761
- [3] Michael Creutz, Taro Kimura, Tatsuhiro Misumi, Aoki Phases in the Lattice Gross-Neveu Model with Flavored Mass terms, Phys.Rev.D83:094506,2011, arXiv:1101.4239,
- [4] Michael Creutz, *Confinement, chiral symmetry, and the lattice*, Acta Physica Slovaca 61, No.1, 1-127 (2011), arXiv:1103.3304,
- [5] P. F. Bedaque, M. I. Buchoff, B. C. Tiburzi and A. Walker-Loud, Phys. Lett. B 662, 449 (2008) [arXiv:0801.3361],
- [6] P. F. Bedaque, M. I. Buchoff, B. C. Tiburzi and A. Walker-Loud, Phys. Rev. D 78, 017502 (2008) [arXiv:0804.1145]
- [7] D. H. Adams, Phys. Rev. Lett. 104, 141602 (2010) [arXiv:0912.2850],
- [8] D. H. Adams, Phys. Lett. B 699, 394 (2011), (2010) [arXiv:1008.2833],
- [9] E.H Saidi et al, *Topological Aspects of Fermions on Hyperdiamond*, LPHE preprint, October 2011,
- [10] L.B Drissi, H. Mhamdi, E.H Saidi, *Anomalous Quantum Hall Effect of 4D Graphene in Background Fields*, JHEP 1110:026,2011, arXiv:1106.5578,
- [11] Michael Creutz, JHEP 04 (2008) 017,[arXiv:0712.1201],
- [12] A.Borici, Phys. Rev. D78 (2008) 074504, [arXiv:0712.4401]
- [13] Michael Creutz, Tatsuhiro Misumi, *Classification of Minimally Doubled Fermions*, Phys.Rev.D82:074502,2010, arXiv:1007.3328,
- [14] S. Capitani, M. Creutz, J. Weber, H.Wittig, JHEP 1009:027,2010, arXiv:1006.2009,
- [15] L.B Drissi, E.H Saidi, M. Bousmina, *Electronic Properties and Hidden Symmetries of Graphene*, Nucl.Phys.B829:523-533,2010, arXiv:1008.4470,

- [16] L.B Drissi, E.H Saidi, M. Bousmina, *Graphene, Lattice QFT and Symmetries*, J. Math. Phys. 52:022306,2011, arXiv:1101.1061
- [17] S. Katz, P. Mayr, C. Vafa, Adv.Theor.Math.Phys. 1 (1998) 53-114, hep-th/9706110,
- [18] A. Belhaj, E.H.Saidi, *On HyperKahler Singularities*, Mod.Phys.Lett. A15 (2000) 1767-1780, arXiv:hep-th/0007143,
- [19] N.C. Leung and C. Vafa; Adv .Theo . Math. Phys 2(1998) 91, hep-th/9711013,
- [20] P. Candelas and X. de la Ossa, “*Comments on Conifolds*,” Nucl. Phys. B342 (1990), 246,
- [21] E. Witten, *Branes and the dynamics of QCD*, Nucl. Phys. B507 (1997) 658, hep-th/9706109
- [22] Harald Nieder, Yaron Oz, *Supergravity and D-branes Wrapping Supersymmetric 3-Cycles*, JHEP 0103:008,2001, arXiv:hep-th/0011288,
- [23] Robbert Dijkgraaf, Lotte Hollands, Piotr Sulkowski, Cumrun Vafa, *Supersymmetric Gauge Theories, Intersecting Branes and Free Fermions*, JHEP 0802:106,2008, arXiv:0709.4446,
- [24] Martijn Wijnholt, F-Theory, GUTs and Chiral Matter, Fortschritte Der Physik-progress of Physics - FORTSCHR PHYS , vol. 58, no. 7-9, pp. 846-854, 2010, arXiv:0809.3878
- [25] Chris Beasley, Jonathan J. Heckman, Cumrun Vafa, GUTs and Exceptional Branes in F-theory - I, JHEP 0901:058,2009, arXiv:0802.3391
- [26] Lalla Btissam Drissi, Leila Medari, El Hassan Saidi, *Quiver Gauge Models in F-Theory on Local Tetrahedron*, arXiv:0908.0471.
- [27] Mohamed Bennai, El Hassan Saidi, *Toric Varieties with NC Toric Actions: NC Type IIA Geometry*, Nucl.Phys.B677:587-613,2004, arXiv:hep-th/0312200,
- [28] Mohamed Bennai, El Hassan Saidi, *NC Calabi-Yau Manifolds in Toric Varieties with NC Torus fibration*, Phys.Lett.B550:108-116,2002, hep-th/0210073,

- [29] El Hassan Saidi, *F-theory on tetrahedron*, Frontiers in Science and Engineering, An International Journal Edited by Hassan II Academy of Science and Technology, Vol 1 (2011) pages 1-24,
- [30] L. H. Karsten, Phys. Lett. B 104, 315 (1981),
- [31] F. Wilczek, Phys. Rev. Lett. 59, 2397 (1987),
- [32] Igor R. Klebanov, Matthew J. Strassler, *Supergravity and a Confining Gauge Theory: Duality Cascade*, HEP 0008:052,2000, arXiv:hep-th/0007191,
- [33] Rachid Ahl Laamara, Lalla Btissam Drissi, El Hassan Saidi, *D-string fluid in conifold: I. Topological gauge model*, Nucl.Phys.B743:333-353,2006, arXiv:hep-th/0604001,
- [34] Rachid Ahl Laamara, Lalla Btissam Drissi, El Hassan Saidi, *D-string fluid in conifold: II. Matrix model for D-droplets on S^3 and S^2* , Nucl.Phys. B749 (2006) 206-224, arXiv:hep-th/0605209,
- [35] El Hassan Saidi, *Topological $SL(2)$ Gauge Theory on Conifold*, African Journal Of Mathematical Physics Vol 5 (2007)57-77, arXiv:hep-th/0601020
- [36] L.B Drissi, E.H Saidi, M. Bousmina, *Four Dimensional Graphene*, Phys.Rev.D84:014504,2011, arXiv:1106.5222,
- [37] Lalla Btissam Drissi, El Hassan Saidi, *On Dirac Zero Modes in Hyperdiamond Model*, Phys.Rev.D84:014509,2011, arXiv:1103.1316,
- [38] El Hassan Saidi, *Tetrahedron in F-theory Compactification*, arXiv:0907.2655,
- [39] Malika Ait Benhaddou, El Hassan Saidi, *Explicit Analysis of Kahler Deformations in 4D $N=1$ Supersymmetric Quiver Theories*, Physics Letters B575(2003)100-110, arXiv:hep-th/0307103
- [40] T. Eguchi, P.B Gilkey, A.J Hanson, *Gravitation Gauge Theories And Differential Geometry*, Physics Reports 66 No 6 pp 213 393 (1980)